

## Calixarene-induced aggregation of perylene bisimides†

Dong-Sheng Guo, Bang-Ping Jiang, Xiang Wang and Yu Liu\*

Received 23rd November 2011, Accepted 24th November 2011

DOI: 10.1039/c2ob06973c

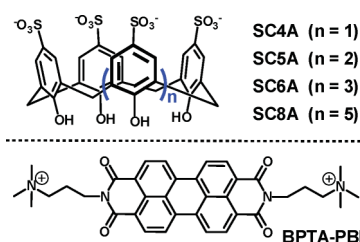
The complex-induced aggregation of perylene bisimides by *p*-sulfonatocalix[*n*]arenes was studied, where the aggregation stability, aggregation distance, as well as the degree of order of aggregation were all improved.

Perylene bisimides (PBIs), a robust kind of photo- and electro-active building block in supramolecular dye chemistry,<sup>1</sup> have shown a wide range of intriguing applications, including liquid crystals,<sup>2</sup> organogels,<sup>3</sup> artificial light harvesting systems,<sup>4</sup> organic electronic devices,<sup>5</sup> and vapor sensing materials.<sup>6</sup> One area of intense interest in recent years has been the development of several other non-covalent forces that can direct the formation of desirable supramolecular architectures,<sup>7</sup> besides the intrinsic  $\pi \cdots \pi$  stacking interaction between PBI backbones. Such supramolecular control over dye arrangement is significant for improving the performance of existing optoelectronic devices and for creating new dye-based materials with tunable optical and electronic properties.<sup>8</sup> Up to now, several non-covalent interactions, such as hydrogen bonding,<sup>9</sup> coordinative bonding<sup>10</sup> and ionic self-assembly,<sup>11</sup> have been employed in the construction of well-defined superstructures.

*p*-Sulfonatocalix[*n*]arenes (SC*n*As, *n* = 4–8), one family of water-soluble calixarene derivatives, possess three-dimensional, flexible,  $\pi$ -electron rich cavities.<sup>12</sup> Consequently, they are promising as versatile macrocyclic receptors that can complex with various kinds of guest molecules.<sup>13</sup> It is particularly fascinating that SC*n*As can induce the aggregation of certain organic dye molecules effectively, exceeding the conventional 1:1 host–guest binding stoichiometry. As an early work, Purrello and coworkers reported that the tetrakis(hydroxycarbonylmethoxy) derivative of SC4A forms complex species with programmable calixarene: porphyrin stoichiometries ranging from 4:1 to 4:7, where the different calixarene: porphyrin complexes are discrete species that do not further self-aggregate.<sup>14</sup> We found that SC*n*A (*n* = 4,5) can induce the oligomerization of 1-pyrenemethylaminium and asymmetric viologen with preferable 1:*n* stoichiometries, which assemble hierarchically into amphiphilic vesicles.<sup>15</sup> Recently, Heyne and Lau found that SC4A can act as a template for forming fluorescent thiazole orange H-aggregates, based on the unexpected complexation yielding 1:3 stoichiometry.<sup>16</sup> As part of our ongoing

program exploiting cavities of SC*n*As, we decided to investigate the complex interaction between SC*n*As and PBI derivatives. Herein, we provide an alternative host–guest strategy that the aggregation capability of PBI is markedly improved by the complexation of calixarene hosts. Our special interest is to increase the stability of PBI stacks and to enhance the degree of order of the stacking molecules, since it has been demonstrated that the charge-carrier mobility, and hence the performance of optoelectronic devices such as field-effect transistors, light-emitting diodes, and photovoltaic cells, depends to a large extent on this parameter.<sup>17</sup>

The structures of calixarene hosts and PBI guest are schematically illustrated in Scheme 1. *N,N'*-bis(propylenetriethylammonium)-3,4,9,10-perylene bisimide (BPTA-PBI) was employed as the model guest molecule, as negatively charged SC*n*As commonly show high binding affinities to organic cations.<sup>13</sup> We preliminarily evaluated the absorption spectra of BPTA-PBI in the absence and presence of 4-phenolsulfonic sodium (PS, the building subunit of SC*n*As) and SC*n*As (*n* = 4, 5, 6, 8) with charge matching equiv. (Fig. 1a). Free BPTA-PBI shows two distinguishable absorption bands, peaked at 500 and 541 nm, respectively, as well as a weak shoulder at 473 nm. The absorptivity at 500 nm is clearly higher than that at 541 nm, reflecting excitonic coupling between adjacent  $\pi$ -stacking PBI backbones.<sup>6d</sup> No appreciable change of BPTA-PBI absorption was observed upon addition of PS as a control experiment. Upon addition of SC*n*As, the absorption bands broadened, the corresponding absorptivities reduced, and especially, the absorption band at 541 nm underwent a bathochromic shift to around 565 nm. The phenomena indicate the stronger electronic coupling between the PBI backbones in the presence of SC*n*As. The fluorescence experiments also prove the strong interactions between BPTA-PBI and SC*n*As. As shown in Fig. 1b, SC*n*As quenched the fluorescence of PBI absolutely to baseline at such a low concentration of 5.0  $\mu$ M. The fluorescence peaked at 547 and



**Scheme 1** Structural illustration of the negatively charged SC*n*As hosts and positively charged BPTA-PBI guest.

Department of Chemistry, State Key Laboratory of Elemento-Organic Chemistry, Nankai University, Tianjin 300071, P. R. China. E-mail: yuliu@nankai.edu.cn; Fax: (+86) 22-2350-3625; Tel: (+86) 22-2350-3625

† Electronic supplementary information (ESI) available: Synthesis of BPTA-PBI, SC*n*As, UV-vis and fluorescence titrations, TEM, SEM, AFM and XRD measurements. See DOI: 10.1039/c2ob06973c

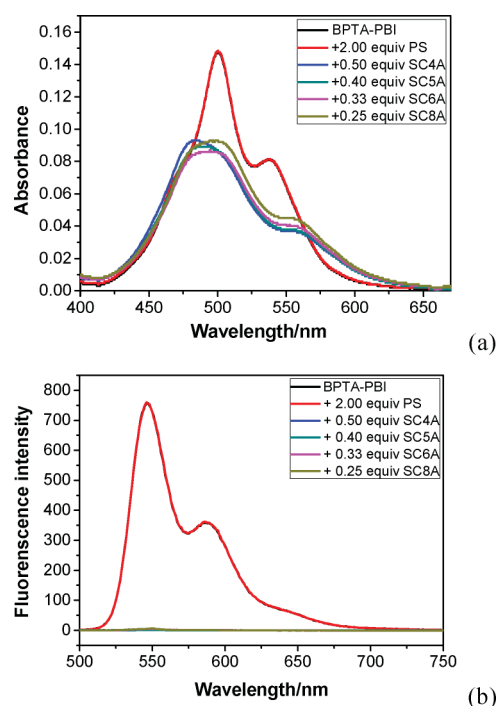


**Fig. 1** UV-vis absorption (a) and fluorescence (b) spectra of free BPTA-PBI (5.0  $\mu\text{M}$ ) and upon addition of PS, SC4A, SC5A, SC6A, and SC8A in water.

587 nm represents the emission of BPTA-PBI monomer, which indicates that there are some unaggregated BPTA-PBI molecules. Upon addition of SCnAs, all the BPTA-PBI molecules were complexed to form aggregates, and therefore, the monomeric fluorescence disappeared.

The complexation behaviors of SCnAs with BPTA-PBI were then studied in detail by UV-vis and fluorescence titrations, as well as Job's plots. Upon gradual addition of SC4A and SC5A into the BPTA-PBI solution (5.0–5.7  $\mu\text{M}$ ), the absorbance decreases gradually, and tends to equilibrium when concentrations of SC4A and SC5A reach 2.0–2.5  $\mu\text{M}$  (Fig. S1a and b). Whereas upon addition of SC6A and SC8A, the absorbance undergoes somewhat complicated changes (Fig. S1c and d), which is possibly ascribed to the relatively flexible and complicated conformations of SC6A and SC8A. Consequently, SC4A and SC5A were selected for quantitative investigation as their preferred stable cone conformations allow the basic precondition to construct supramolecular nanoarchitectures with well-defined geometries.<sup>18</sup> Prior to the quantitative curve-fitting, it was necessary to ascertain the host-guest binding stoichiometries, for which the Job method was employed. As can be seen from Fig. 2, the Job plots performed for BPTA-PBI with SC4A and SC5A show the maximum values of  $\Delta A$  (complex-induced changes of absorbance) at the BPTA-PBI molar fractions of 0.68 and 0.72, which indicate that the binding stoichiometries of SC4A and SC5A with BPTA-PBI are 1 : 2 and 2 : 5, respectively. The host-guest binding ratios can also be observed from the UV-vis and fluorescence titration results (Fig. S1 and S2). It is noticeable that the obtained host-guest stoichiometries are significantly satisfied to charge matching between sulfonate groups and quaternary ammonium groups.

We can see from the UV-vis spectra (Fig. 1a) that free BPTA-PBI molecules exist mainly in the aggregated form, indicating that

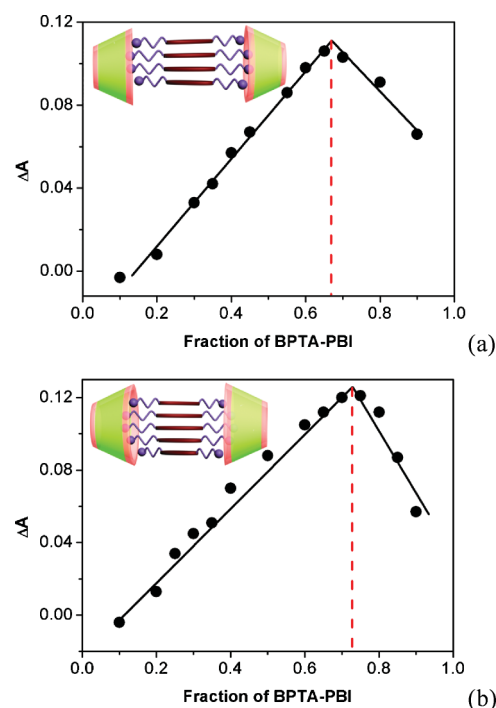
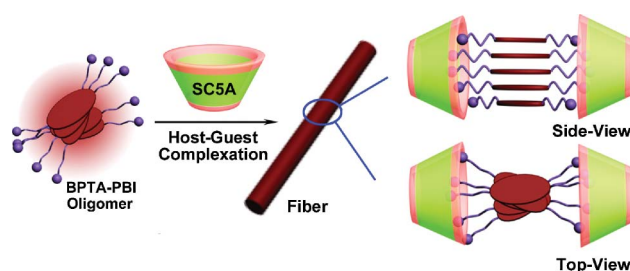


**Fig. 2** Job plots for SC4A (a) and SC5A (b) upon complexation with BPTA-PBI in water. Absorption changes recorded at 500 nm. The sum of the total concentrations of BPTA-PBI and calixarenes is constant (10.0  $\mu\text{M}$ ).

SCnAs should bind with the BPTA-PBI oligomer, but not the monomer. Consequently, by assuming two BPTA-PBI molecules as one binding unit for simplicity, we calculated the obvious binding stability constant ( $K_s$ ) of SC4A with BPTA-PBI as  $1.8 \times 10^6 \text{ M}^{-1}$  utilizing nonlinear least-squares analysis of the UV-vis spectral titration data by the isodesmic or equal-K model (eqn 1, Fig. S3). The  $K_s$  value of SC5A with BPTA-PBI was obtained as  $5.9 \times 10^6 \text{ M}^{-1}$  in the same manner, by assuming two and half BPTA-PBI molecules as one binding unit. The  $K_s$  values are 2–3 orders of magnitude larger than those with quaternary ammonium guests (in the region of  $10^3$ – $10^4 \text{ M}^{-1}$ ).<sup>13</sup> This is mainly owing to the multiple interactions that occur when 4–5 quaternary ammonium groups are simultaneously bound to SC4A and SC5A.

The SCnA-induced aggregation of BPTA-PBI is illustrated in Scheme 2. In the present experimental conditions of 5.0  $\mu\text{M}$  aqueous solution, free BPTA-PBI exists in aggregated form according to the UV-vis result. We have tried to evaluate the



**Scheme 2** Schematic illustration of the complex-induced aggregation of BPTA-PBI by SC5A.

aggregation constant of BPTA-PBI, but it is too strong to be obtained by the concentration-dependent UV-vis spectra. BPTA-PBI exists theoretically in monomer form at lower concentration ( $<5.0 \mu\text{M}$ ), however unfortunately, it can be hardly monitored owing to its limited absorbance. As a result, we cannot calculate its average aggregation number in the absence of aggregation constant. We further performed the DLS measurement of BPTA-PBI at a concentration of  $5.0 \mu\text{M}$ , showing no appreciable scattering intensity, which implies that no large-size aggregate was formed. Combining the UV-vis and DLS results together, we infer that free BPTA-PBI exists in oligomer. Upon addition of SC4A and SC5A, DLS results show that the complexes form spectacular aggregates, giving average hydrodynamic diameters of 191 nm for SC4A and 200 nm for SC5A. Two size distributions were observed in both processes (Fig. 3), where the small one can be attributed to the formation of the complexation-induced aggregate fibers, and the large one originates from the further assembly of calixarenes. The aggregate morphology of the SC5A + BPTA-PBI complex was further characterized by TEM, SEM and AFM. The TEM image of free BPTA-PBI shows some irregular arrangement without specific topological structure (Figure S4), whereas the TEM image of the SC5A + BPTA-PBI complex shows nano-rod structures with an average length of 220 nm (Fig. 4a). These rods are considered to be comprised of bundles of fibers, resulting from the hierarchical assembly of calixarenes. Such  $\pi$ -stacking assembly of SCnAs in the solid-state has been extensively studied.<sup>12b</sup> The regular linear arrangements of micron magnitude were observed from the AFM image (Fig. 4c), which indicates that the discotic BPTA-PBI molecules self-assemble into columnar stacks upon complexation with SC5A, representing one kind of supramolecular polymer driven concurrently by two complementary interactions,  $\pi \cdots \pi$  stacking and ionic self-assembly. Ionic self-assembly is characteristic of a cooperative binding mechanism, that is, primary interactions stimulate further secondary interactions, which propagate toward the final self-assembly structures.<sup>11</sup> In the present case, free BPTA-PBI forms oligomers *via* mere  $\pi \cdots \pi$  stacking interactions between perylene backbones. Upon addition of SCnAs, both host-guest and electrostatic interactions are involved, boosting the  $\pi \cdots \pi$  stacking interactions pronouncedly. The synergetic contribution

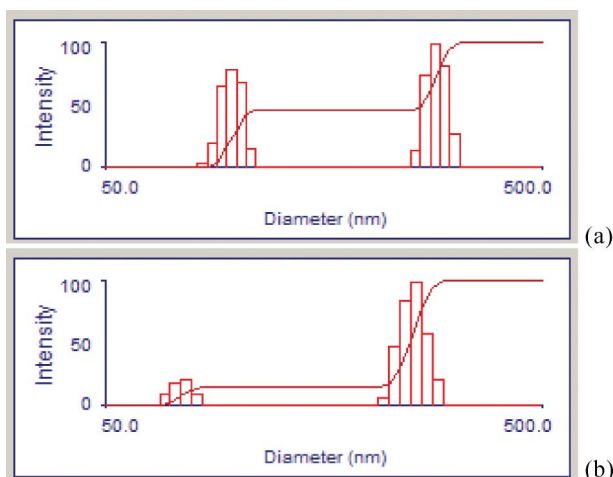


Fig. 3 DLS for SC4A (a) and SC5A (b) upon complexation with BPTA-PBI in water.

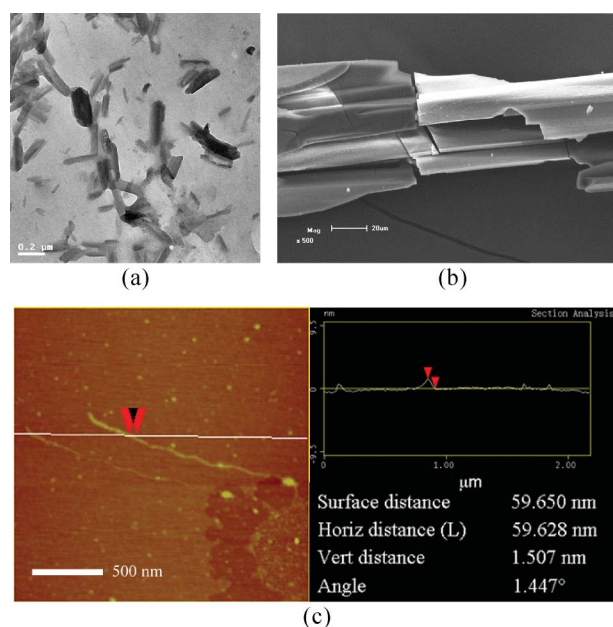


Fig. 4 TEM (a), SEM (b) and AFM (c) images of the SC5A + BPTA-PBI complex.

of these driving forces leads ultimately to the hierarchical well-defined superstructures. Moreover, SEM measurement also gave evidence of highly ordered structures (Fig. 4b).

XRD measurements were performed to investigate the  $\pi \cdots \pi$  stacking distances of BPTA-PBI in the absence and presence of SC4A and SC5A (Fig. S5). The obtained results show that the  $\pi \cdots \pi$  stacking distance of free BPTA-PBI is  $3.54 \text{ \AA}$ , and the distances of the SC4A and SC5A complexes are  $3.42$  and  $3.39 \text{ \AA}$ , respectively. The  $\pi$ -stacking aggregation of BPTA-PBI becomes more compact upon complexation with SC4A and SC5A. The shortened  $\pi \cdots \pi$  stacking distance also indicates the improved aggregation capability, in accordance with the above UV-vis results, which can further explain why the SCnA + BPTA-PBI complexes form large-size aggregates, while free BPTA-PBI forms only oligomer.

In summary, we investigated the complex-induced aggregation of PBI by SCnAs, and the aggregation property of PBI is pronouncedly improved from the aspects of aggregation stability and aggregation distance, as well as the degree of order of aggregation. All these points are crucial for exploring the desired optical and electronic properties of well-defined materials. In addition, the present SCnA + PBI assemblies are considered to be a novel kind of supramolecular zwitterionic conjugated polyelectrolyte, showing promising potential as organic field-effect transistors, where the unwanted motion of counterions in conventional cationic conjugated polyelectrolytes can be effectively avoided.<sup>19</sup> Further studies of the performance of organic field-effect transistors based on calixarene-peryene complexes are currently under investigation.

## Acknowledgements

We thank 973 Program (2011CB932502), NSFC (20932004, 21172119) for financial support.

## Notes and references

- 1 (a) F. Würthner, *Chem. Commun.*, 2004, 1564–1579; (b) Z. Chen, A. Lohr, C. R. Saha-Möller and F. Würthner, *Chem. Soc. Rev.*, 2009, **38**, 564–584; (c) L. Zang, Y. Che and J. S. Moore, *Acc. Chem. Res.*, 2008, **41**, 1596–1608.
- 2 O. Thiebaut, H. Bock and E. Grelet, *J. Am. Chem. Soc.*, 2010, **132**, 6886–6887.
- 3 F. Würthner, C. Bauer, V. Stepanenko and S. Yagai, *Adv. Mater.*, 2008, **20**, 1695–1698.
- 4 F. C. De Schryver, T. Vosch, M. Cotlet, M. Van der Auweraer, K. Müllen and J. Hofkens, *Acc. Chem. Res.*, 2005, **38**, 514–522.
- 5 (a) A. Kraft, A. C. Grimsdale and A. B. Holmes, *Angew. Chem., Int. Ed.*, 1998, **37**, 402–428; (b) R. T. Weitz, K. Amsharov, U. Zschieschang, E. B. Villas, D. K. Goswami, M. Burghard, H. Dosch, M. Jansen, K. Kern and H. Klauk, *J. Am. Chem. Soc.*, 2008, **130**, 4637–4645.
- 6 (a) Y. Che, X. Yang, S. Loser and L. Zang, *Nano Lett.*, 2008, **8**, 2219–2223; (b) Y. Che and L. Zang, *Chem. Commun.*, 2009, 5106–5108; (c) Y. Liu, K.-R. Wang, D.-S. Guo and B.-P. Jiang, *Adv. Funct. Mater.*, 2009, **19**, 2230–2235; (d) B.-P. Jiang, D.-S. Guo and Y. Liu, *J. Org. Chem.*, 2010, **75**, 7258–7264.
- 7 (a) C. Ehli, C. Oelsner, A. Mateo-Alonso, M. Prato, C. Schmidt, C. Backes, F. Hauke, A. Hirsch and D. M. Guldi, *Nat. Chem.*, 2009, **1**, 243–249; (b) E. Krieg, E. Shirman, H. Weissman, E. Shimon, S. G. Wolf, I. Pinkas and B. Rybtchinski, *J. Am. Chem. Soc.*, 2009, **131**, 14365–14373; (c) J.-H. Ryu, C.-J. Jang, Y.-S. Yoo, S.-G. Lim and M. Lee, *J. Org. Chem.*, 2005, **70**, 8956–8962.
- 8 F. J. M. Hoeben, P. Jonkheijm, E. W. Meijer and A. P. H. J. Schenning, *Chem. Rev.*, 2005, **105**, 1491–1546.
- 9 (a) C. Thalacker and F. Würthner, *Adv. Funct. Mater.*, 2002, **12**, 209–218; (b) A. P. H. J. Schenning, J. van Herrikhuyzen, P. Jonkheijm, Z. Chen, F. Würthner and E. W. Meijer, *J. Am. Chem. Soc.*, 2002, **124**, 10252–10253; (c) T. Seki, A. Asano, S. Seki, Y. Kikkawa, H. Murayama, T. Karatsu, A. Kitamura and S. Yagai, *Chem.–Eur. J.*, 2011, **17**, 3598–3608.
- 10 (a) C.-C. You and F. Würthner, *J. Am. Chem. Soc.*, 2003, **125**, 9716–9725; (b) G. Golubkov, H. Weissman, E. Shirman, S. G. Wolf, I. Pinkas and B. Rybtchinski, *Angew. Chem., Int. Ed.*, 2009, **48**, 926–930.
- 11 (a) Y. Guan, Y. Zakrevskyy, J. Stumpe, M. Antonietti and C. F. J. Faul, *Chem. Commun.*, 2003, 894–895; (b) Y. Zakrevskyy, C. F. J. Faul, Y. Guan and J. Stumpe, *Adv. Funct. Mater.*, 2004, **14**, 835–841; (c) T. Ma, C. Li and G. Shi, *Langmuir*, 2008, **24**, 43–48.
- 12 (a) S. Shinkai, S. Mori, H. Koreishi, T. Tsubaki and O. Manabe, *J. Am. Chem. Soc.*, 1986, **108**, 2409–2416; (b) J. L. Atwood, L. J. Barbour, M. J. Hardie and C. L. Raston, *Coord. Chem. Rev.*, 2001, **222**, 3–32; (c) F. Perret, A. N. Lazar and A. W. Coleman, *Chem. Commun.*, 2006, 2425–2438.
- 13 D.-S. Guo, K. Wang and Y. Liu, *J. Incl. Phenom. Macrocycl. Chem.*, 2008, **62**, 1–21.
- 14 (a) L. D. Costanzo, S. Geremia, L. Randaccio, R. Purrello, R. Lauceri, D. Sciotto, F. G. Gulino and V. Pavone, *Angew. Chem., Int. Ed.*, 2001, **40**, 4245–4247; (b) G. Moschetto, R. Lauceri, F. G. Gulino, D. Sciotto and R. Purrello, *J. Am. Chem. Soc.*, 2002, **124**, 14536–14537; (c) F. G. Gulino, R. Lauceri, L. Frish, T. Evan-Salem, Y. Cohen, R. D. Zorzi, S. Geremia, L. D. Costanzo, L. Randaccio, D. Sciotto and R. Purrello, *Chem.–Eur. J.*, 2006, **12**, 2722–2729.
- 15 (a) K. Wang, D.-S. Guo and Y. Liu, *Chem.–Eur. J.*, 2010, **16**, 8006–8011; (b) K. Wang, D.-S. Guo, X. Wang and Y. Liu, *ACS Nano*, 2011, **5**, 2880–2894.
- 16 V. Lau and B. Heyne, *Chem. Commun.*, 2010, **46**, 3595–3597.
- 17 (a) See Special Issue on Molecular Conductors: *Chem. Rev.*, 2004, **104**; (b) F. C. Grozema and L. D. A. Siebbeles, *Int. Rev. Phys. Chem.*, 2008, **27**, 87–138; (c) D. Gonzalez-Rodriguez and A. P. H. J. Schenning, *Chem. Mater.*, 2011, **23**, 310–325.
- 18 D.-S. Guo, K. Chen, H.-Q. Zhang and Y. Liu, *Chem.–Asian J.*, 2009, **4**, 436–445.
- 19 (a) J. Fang, B. H. Wallikewitz, F. Cao, G. Tu, C. Müller, G. Pace, R. H. Friend and W. T. S. Huck, *J. Am. Chem. Soc.*, 2011, **133**, 683–685; (b) U. Scherf, *Angew. Chem., Int. Ed.*, 2011, **50**, 5016–5017.